The Journal of Neuroscience, May 1, 1996, *16*(9):3056–3066

High-Frequency Oscillations in the Output Networks of the Hippocampal–Entorhinal Axis of the Freely Behaving Rat

James J. Chrobak and Gyorgy Buzsáki

Center for Molecular and Behavioral Neuroscience, Rutgers, The State University of New Jersey, Newark, New Jersey 07102

Population bursts of the CA3 network, which occur during eating, drinking, awake immobility, and slow-wave sleep, produce a large field excitatory postsynaptic potential throughout stratum radiatum of the CA1 field (sharp wave). The CA3 burst sets into motion a short-lived, dynamic interaction between CA1 pyramidal cells and interneurons, the product of which is a 200 Hz oscillatory field potential (ripple) and phase-related discharge of the CA1 network. Although many CA1 pyramidal neurons discharge during the time frame (50–100 msec) of each sharp wave, each wave of a ripple (~5 msec) reflects the synchronization of more discrete subsets of CA1 neurons.

When we used multi-site recordings in freely behaving rats, we observed ripples throughout the longitudinal extent (~4–5 mm) of the dorsal CA1 region that were coherent for multiple cycles of each ripple. High-frequency ripples were also observed throughout the hippocampal–entorhinal output pathway that were concurrent but less coherent on a cycle-by-cycle basis. Single and multiunit neuronal activity was phase-related to local ripples throughout the hippocampal–entorhinal output pathway. Entorhinal ripples occurred 5–30 msec after the CA1 ripples and were related to the occurrence of an entorhinal sharp wave. Thus, during each hippocampal sharp wave, there is a powerful synchronization among the neuronal networks that connect the hippocampus to the neocortex. We suggest that this population interaction (1) biologically constrains theoretical models of hippocampal function and dysfunction and (2) has the capacity to support an "off-line" memory consolidation process.

Key words: hippocampus; subiculum; entorhinal cortex; oscillations; sharp waves; memory; epilepsy

The hippocampus and entorhinal cortex (EC) are substrates for the formation of enduring memories and the etiology/pathology of Alzheimer's dementia as well as temporal lobe epilepsy. The manner and mechanisms by which these structures interact have implications for both physiological and pathophysiological processes.

Synchronous population potentials and localized oscillatory patterns occur in many neural networks (Buzsáki et al., 1983, 1992; Steriade et al., 1993; Freeman and Barrie, 1994; Gray, 1994; Singer, 1994). These events reflect synchronizing mechanisms for coordinating ensembles of neurons within distributed neural networks and for bringing neuronal aggregates within/across structures together in time (Buzsáki and Chrobak, 1995).

The physiology of the hippocampal–entorhinal networks is characterized by behaviorally regulated, macroscopic potentials that temporally organize specific subsets of network neurons. θ occurs during exploratory behavior and rapid eye movement sleep and represents a period when hippocampal circuits receive rhythmic input from neurons within the superficial layers of the EC (Mitchell and Ranck, 1980; Buzsáki et al., 1983; Boeijinga and Lopes da Silva, 1988; Stewart et al., 1992). In contrast, during sharp waves, which occur during consummatory behaviors and slow-wave sleep, the output neurons of the hippocampus and EC participate in organized population bursts (Buzsáki, 1989; Chrobak and Buzsáki, 1994; Ylinen et al., 1995). These patterns seem to serve companion processes. θ synchronizes the input pathway into the hippocampus, whereas sharp waves synchronize the output pathway from the hippocampus back to neocortical structures. Each potential is associated with more localized oscillatory field potentials that reflect the temporal organization of neuronal subsets within 5–25 msec (Bragin et al., 1995; Buzsáki and Chrobak, 1995; Ylinen et al., 1995).

The sharp wave is a large amplitude (1–3 mV), aperiodic, field potential observed most prominently in stratum radiatum of the CA1 region (Buzsáki et al., 1983; Buzsáki, 1986; Suzuki and Smith, 1987). Released from inhibitory constraints associated with θ (Leung and Yim, 1986; Fox, 1989; Soltész and Deschénes, 1993), the highly interconnected CA3 network exhibits population bursts. The burst of the CA3 network produces a field excitatory postsynaptic potential (EPSP) (a sharp wave) in the target of the CA3 Schaffer collaterals, the dendrites of CA1 pyramidal cells, and interneurons. The massive depolarization of CA1 sets into motion a short-lived, dynamic interaction between these cell populations. The product of this interaction is an oscillatory field potential (ripple) within stratum pyramidale and a phase-related discharge of the CA1 network at 200 Hz (Buzsáki et al., 1992). The synaptic currents mediating the ripple are rhythmic inhibitory postsynaptic potentials (IPSPs) near the soma of CA1 neurons produced by a high-frequency discharge of CA1 basket cells and other interneurons (Ylinen et al., 1995). Although interneurons discharge at a high frequency, CA1 pyramidal cells, excited by the CA3 input yet constrained by the interneuron barrage, typically fire once or not at all. Throughout the entire CA1 network,

Received Nov. 30, 1995; revised Jan. 18, 1996; accepted Jan. 22, 1996.

This work was supported by the National Institutes of Health (NS34994, 1P41RR09754), National Science Foundation, Human Frontiers Science Project, the Whitehall Foundation (G.B.), and the Alzheimer's Association (J.J.C.). We thank Drs. H. Read and A. Bragin for all their help, comments, and discussion, and K. Wise and J. Hetke for supplying silicon probes.

Correspondence should be addressed to Gyorgy Buzsáki, CMBN, Rutgers University, 197 University Avenue, Newark, NJ 07102.

however, a large number of pyramidal cells reach discharge threshold on each ~5 msec wave of the ripple.

The present study examined the interaction between this synchronized output of CA3–CA1 and the output neurons of a larger integrated network that includes the subiculum and deep layers of the presubiculum, parasubiculum, and EC. We found that similar to the CA1 region, each output population of the hippocampal–entorhinal network produces an organized, short-lived, fast oscillation of their discharging neurons concurrent with CA1 ripples.

MATERIALS AND METHODS

Animals and surgery. Twenty-four adult Sprague–Dawley rats were used in the following experiments. For surgery, rats were anesthetized with a ketamine cocktail (4 ml/kg) consisting of 25 mg/ml ketamine, 1.3 mg/ml xylazine, and 0.25 mg/ml acepromazine. After a midline scalp incision, two to four burr holes were drilled in the skull over the hippocampal and retrohippocampal cortices. Two or three sets of four 50 μm tungsten wires were positioned into the dorsal hippocampus/subicular regions [anterior-posterior (AP), −2.5, −5.0, −7.5 from bregma; medial-lateral (ML), 1.5, 2.5, 4.0; dorsal-ventral (DV), 2.0–4.0 from the skull and above retrohippocampal regions (AP, −7.5–9.0; ML, 3.0–5.0)]. One or more sets were chronically fixed, whereas the other was attached to a drive consisting of a brass post and a single machine screw. The latter allowed for optimal, postsurgical positioning of electrodes. One or two single tungsten microelectrodes (0.5–3.0 MΩ) mounted to similar drives were positioned over either or both retrohippocampal areas (AP, −7.5–9.0; ML, 3.0–5.0). These mounts allowed for the slow passage of the microelectrode through the retrohippocampal region. In two animals, a 16-channel silicon probe (100 μm tip separations) (Bragin et al., 1995) was positioned via a movable microdrive into the EC. A pair of 150 μm wires were also positioned in the angular bundle (AP, 7.2; ML, 4.2; DV, 4.0) or CA3 region (AP, 4.0; ML, 4.0; DV, 4.0) for stimulation. Two stainless steel watchscrews driven into the bone above the cerebellum served as indifferent and ground electrodes. Two or more additional support screws were positioned, and the entire ensemble was secured to the skull with dental acrylic. All electrodes—indifferent, ground, and stimulating—were attached to male pins that were secured in a rectangular 3 × 4 pin array and secured with dental acrylic.

Recording. Bioelectrical activity was recorded in the freely behaving rats during movement, awake immobility, or distinct sleep stages. The headstage of the animal (male pins) was connected to sixteen MOSFET-input operational amplifiers mounted in a female connector. This direct amplification at the headstage serves to eliminate cable movement artifacts (Buzsáki et al., 1989). An attached cable fed into a rotating swivel (Biela, Irvine, CA) allowed for the free rotation of the recording cable and movement of the rodent within a standard plexiglas home cage. An amplifier system (Grass Neurodata Acquisition System, Quincy, MA) and an analog-to-digital hard/software system (RC Electronics, Santa Barbara, CA) run on a PC computer allowed for direct visualization and storage of electrical activity. Wide band signals (1 Hz–5 kHz) were sampled at 10 kHz (100 μsec) and stored on optical disks.

After optimization of hippocampal microelectrodes for detection of ripples (200 Hz oscillations) within stratum pyramidale of CA1 and sharp waves within stratum radiatum of CA1, the tungsten microelectrode or multielectrode 50 μm wires were lowered through retrohippocampal structures. Discriminable units and/or prominent oscillations were recorded during both sharp waves (awake immobility) and θ states (locomotor activity and paradoxical sleep); 100–400 (400 msec) epochs triggered by the occurrence of a sharp wave and/or ripple were recorded. When possible (depending on the stability of unit recording), additional continuous epochs (30–90 sec) were recorded during both sharp waves and θ states. When prominent retrohippocampal oscillations or a prominent retrohippocampal sharp potential was observed, additional epochs triggered by the occurrence of these events were recorded. After completion of a single pass of the movable microelectrode(s), rats were anesthetized with pentobarbital and perfused with the electrode *in situ.*

Data processing and analysis. Unit activity and field potentials were filtered digitally (120 dB/octave: unit, band pass 0.5–5.0 kHz; high-frequency ripples, band pass 100–400 Hz) and analyzed off-line on a 486/33 or an IBM RS 6000 computer or both. Putative single units were verified by the absence of spikes ≥1 msec (typically >3–5× baseline amplitude) in autocorrelograms, reflecting the refractory period. Remaining unit activity (units >2× baseline, with interspike intervals <1 msec) were considered multiunit. Ripple peaks were detected after off-line filtering (100–400 Hz), using a peak-detection algorithm.

Single and multiunit activity were cross-correlated with local ripple peaks and local ripple peaks with CA1 ripples, using the ripple peaks as the zero reference point. Local field averages were obtained by averaging wide-band and filtered signals, using ripple peaks or unit pulses as the zero reference.

Histology. Tissue was processed using either thionin stain or a modified silver method that allows for direct visualization of damaged neurons (Gallyas et al., 1990). The latter technique allowed for more direct visualization, and thus localization, of neurons at the electrode tip. Briefly, after completion of the experiments, the rats were anesthetized deeply and perfused through the heart with cacodylate-buffered saline, pH 7.5, followed by a cacodylate-buffered fixative containing 4% paraformaldehyde and 5.9% calcium chloride, pH 7.5. Brains were left *in situ* for 24 hr, removed, and then postfixed in the same solution for 1 week. The brains were sectioned on a vibratome at 80 μm, dehydrated with propanol, and placed in an esterifying solution (98% propanol, 1.2% sulfuric acid) at 56°C for 16 hr. After rehydration and sectioning, they were processed according to the following procedure: (1) pretreatment in 8% acetic acid for 10 min, (2) washing in water for 1 min, (3) physical development with tungstosilicic acid for ~10 min, and (4) washing in 1% acetic acid. Finally, the sections were dehydrated, mounted on slides, and coverslipped.

RESULTS

Coupling of CA1 ripples along the long axis of the hippocampus

Transient high frequency oscillations (ripples) at ~200 Hz were observed as electrodes traversed near the CA1 pyramidal cell layer coincident with hippocampal sharp waves. CA1 ripples are defined as a series of 5–15 oscillatory waves of varying amplitude/duration with a peak-to-peak time of ~5 msec (Figs. 1, 2). Our measurements along the longitudinal axis of the hippocampus indicate that several cycles (three to five) of the dynamically developing CA1 ripples are coherent along this dimension for distances of 4–5 mm ($n = 6$; Fig. 1*E*). It is important to note that the waxing and waning of CA1 ripples is a localized phenomenon, which is likely to represent the local development of synchrony among subpopulations of CA1 interneurons. Figure 2 illustrates that although distant sites within the dorsal CA1 region are on average coherent over several cycles of a ripple, ripples at specific sites can occur quite independently. Although the absence of a prominent ripple in the contralateral hippocampus was not unusual, occurring 30–50% (Fig. 2*C*), the absence of a prominent ipsilateral ripple was rare (<5%; Fig. 2*B*). Ripples developed in both hemispheres of the hippocampus virtually simultaneously, with cross-correlograms demonstrating peak occurrence near the zero-reference ripple; however, there was no cycle-by-cycle synchrony between ripples in the contralateral hippocampus (Fig. 1*F*).

Coupling of retrohippocampal neurons to local field, and CA1 ripples

While examining the relationship between CA1 ripples and the discharge of retrohippocampal neurons, we observed prominent local field oscillations within the subicular and deep layer presubicular, parasubicular, and entorhinal cortices. We examined the relationship between these retrohippocampal ripples and unit discharge as well as the relationship of the retrohippocampal ripples to CA1 ripples. Given that principle neurons discharge only on some limited number of local ripple events, ripple–ripple cross-correlograms yield a more accurate reflection of population synchrony between CA1 neurons and retrohippocampal neurons.

At all sites within the hippocampal–entorhinal output network where high-frequency ripples could be observed, single and mul-

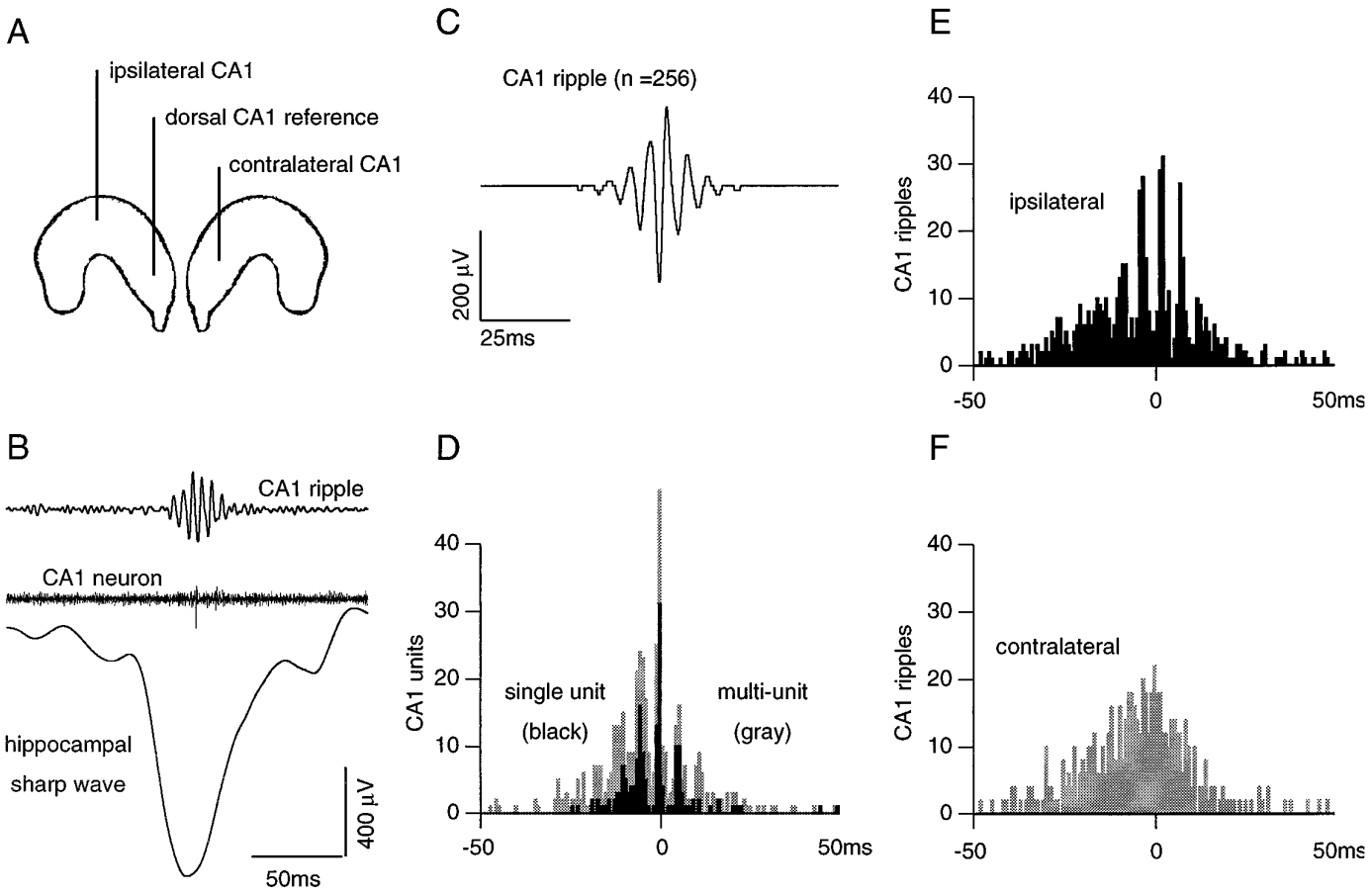

Figure 1. CA1 ripple and associated neuronal events in the ipsilateral and contralateral CA1 regions. *A,* Recording locations in ipsilateral and contralateral CA1 regions of hippocampus. *B,* Hippocampal sharp wave is a synchronized field EPSP in the apical dendritic targets of the CA3 Schaffer collateral input. This depolarization sets into motion a short-lived population interaction between CA1 pyramidal cells and interneurons whose product is an oscillatory field potential (200 Hz) and phase-related discharge of CA1 neurons. Typically, a CA1 pyramidal cell fires a single spike in association with a local ripple (as shown). *Upper* and *middle traces,* recording from pyramidal layer (100–400 Hz and 0.5–5.0 kHz, respectively). *Bottom trace,* simultaneously recorded field potential (1–50 Hz) from stratum radiatum. *C,* Average ripple recorded in septal extent of the dorsal CA1 region. Relationship between negative peak of CA1 ripple (as shown in *C*) and locally recorded single and multiunit (*D*) activity and CA1 ripples recorded in the ipsilateral (*E*) and contralateral hippocampus (*F*). Note that ripples with the ipsilateral dorsal CA1 region are coherent for three to four cycles of the oscillation, whereas those recorded in the contralateral hippocampus are not.

tiunit activity was correlated to the negative phase of the local field oscillation (Figs. 3, 4, 5), although the degree of modulation for multiple cycles of the oscillation varied from site to site. This variation is likely to depend on the position of the recording electrode within the synaptic field generating the ripple, which may not be optimal for recording well isolated units, as well the number of times a neuron discharges during any given ripple. Thus, for example, the subicular neuron illustrated in Figure 3 seems better modulated because this neuron tended to fire more than once, often exhibiting multiple spikes, on any given ripple with which it discharged.

Figure 3 illustrates that ripples in the ipsilateral dorsal subiculum were coherent with CA1 ripples for multiple cycles ($n = 4$; Fig. 3*B*), as was observed at sites across the dorsal CA1 region. Ripples at contralateral subicular sites occurred concurrently but were not coherent on a cycle-by-cycle basis (Fig. 3*B*). Both single ($n = 13$) and multiunit subicular unit activity were phase-related to the negative peaks of these local high-frequency oscillations (Fig. 3).

High-frequency ripples were also observed near the deep layers of the presubiculum. Figure 4 illustrates the relation of presubicular ripples to an ipsilateral CA1 ripple. Note the qualitative decrement in cycle-by-cycle coherence in the ripple–ripple cross-correlogram (Fig. 4*B*), although the peak of the cross-correlogram indicates that these dynamically developing events occur virtually simultaneously in both structures. The peaks of ripple–ripple cross-correlograms did not indicate any significant (>5 msec or a single cycle) lag in the occurrence of presubicular ripples as compared with CA1 ripples (Fig. 4*B*). Single presubicular ($n = 8$) and multiunit neurons recorded at all sites within the deepest layers near the overlying white matter were modulated powerfully by local high-frequency oscillations (Fig. 4*A,D*), discharging on the negative peak of the local oscillation.

Entorhinal ripples were more variable and exhibited fewer oscillatory waves per ripple (Figs. 5*A*, 6). Although an occasional entorhinal ripple preceded the occurrence of CA1 ripples, the majority (~95%) occurred either virtually simultaneously (±5 msec) or were delayed (>5–30 msec peak-amplitude wave to peak-amplitude wave) as compared with a dorsal CA1 site (Figs. 5*A,D*; 6*A,D*).

Entorhinal and parasubicular single and multiunit activity were phase-related to local ripples, although the degree of oscillatory

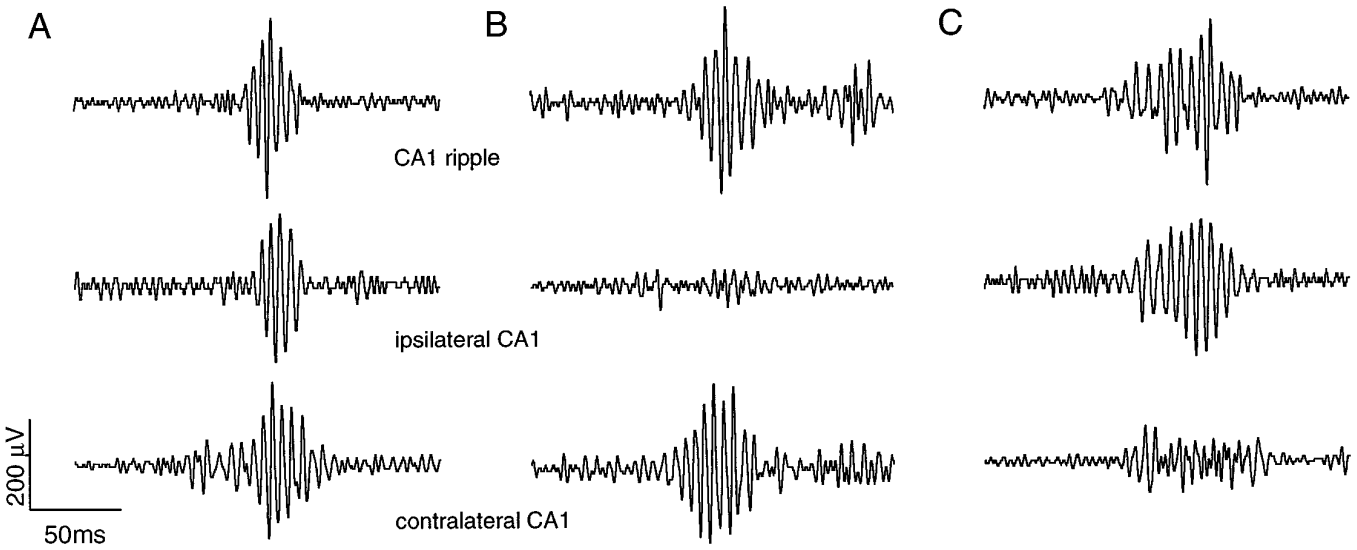

Figure 2. Ripples at various positions with the CA1 region can emerge independently. *A, B, C,* Single 200 msec traces recorded concurrently in the ipsilateral (~5 mm distance from reference CA1 ripple) and contralateral CA1 pyramidal cell region. Ripples typically occur concurrently at various sites within CA1 (*A*), but the occurrence, amplitude, and duration can be independent at various sites within CA1 (*B, C*).

modulation was clearly less than at CA1, subicular, or presubicular sites (Fig. 5*A,D*). Entorhinal neurons were phase-related to the negative peak of the local oscillation ($n = 17$), with several neurons ($n = 6$) exhibiting two or three oscillatory peaks in their cross-correlogram (Fig. 5*D*). It also was observed that the peak amplitude entorhinal oscillations were not the most prominent within layers V–VI, but were better expressed in the most superficial aspect of layers V, IV, and III.

Entorhinal ripples, observed as electrodes penetrated layers V–VI and entered the broad expanse of layer III, were associated with a prominent negative-going wave that we refer to as entorhinal sharp waves (Figs. 6, 7). This slow potential reversed in polarity near layer II, suggesting that it represents a synchronized field EPSP in the apical dendritic zone of layer V–VI neurons. This entorhinal sharp wave is similar to that described previously by Paré and colleagues (1995) in the cat. These authors also observed that deep layer EC neurons discharge regularly in association with these events, whereas superficial neurons discharged much less frequently.

Figure 7 illustrates the relationship between entorhinal ripples and their associated entorhinal sharp waves to the hippocampal CA1 ripple. Correlations were observed between the occurrence of these entorhinal sharp waves and CA1 ripples in all animals (Figs. 6, 7); however, there was an obvious variability in degree of concurrence of these field events. This variation may represent differences in the topographical innervation of the EC from CA1. The topography of CA1 to the EC is such that the septal CA1 and subiculum project more to the lateral aspect of the EC, whereas the temporal CA1 projects to the more medial aspect of the EC (Amaral and Witter, 1995). We have a limited sample over the rostral-caudal, medial-lateral dimension, and although Figure illustrates a prominent relationship between dorsal CA1 and the caudal-medial extent of the EC, additional studies will be needed to define the topography of the observed physiological connectivity.

DISCUSSION

The present study demonstrates novel findings that integrate the ripple-related discharge of CA1 neurons during hippocampal sharp waves with electrophysiological events occurring throughout the output networks of the hippocampal–entorhinal axis. First, during hippocampal sharp waves, local field oscillations are synchronous throughout the dorsal CA1 region, as well as in the subicular and deep layers of the presubicular, parasubicular, and entorhinal cortices. Second, throughout the hippocampal–entorhinal output network, discharge of neurons synchronized to the negative peak of locally developing ripples in each region. Third, entorhinal ripples are associated with a negative-going entorhinal sharp wave that reverses in polarity near the border of layers II–III. This latter phenomenon may reflect the synchronized depolarization of the apical dendritic field of layer V–VI neurons by the hippocampal sharp wave-related discharge of CA1, subiculum, and presubiculum neurons that synapse in this region.

Thus, in association with hippocampal sharp waves, highly organized discharges occur throughout the entire output network of the hippocampal–entorhinal axis. These organized discharges bring tens of thousands of neurons within these interconnected networks together so that they discharge in discrete subsets on each of several high-frequency oscillatory waves. This coordinated population output is likely to have a potent impact on many forebrain targets.

Temporal structure in hippocampal–entorhinal neuronal networks: a role for interneurons

Our observations demonstrate that in association with hippocampal sharp waves, there are locally developing field oscillations throughout the output network of the hippocampal–entorhinal axis. The extracellulary recorded oscillatory fields may reflect synchronous membrane oscillations in pyramidal neurons caused by rhythmic IPSPs. Previous findings demonstrate that the 200 Hz field oscillation observed within CA1 reflects synchronized IPSPs in the perisomatic region of CA1 neurons (Ylinen et al., 1995). Networks of interneurons can achieve rhythmic, synchronous population discharges, which then exert a hyperpolarizing oscillation on the membrane potential of pyramidal neurons (Michelson and Wong, 1994; Whittington et al., 1995; Traub et al., in press). Such oscillations, occurring in the context of a depolarizing input, can impose a periodic fluctuation in the pyramidal cell membrane

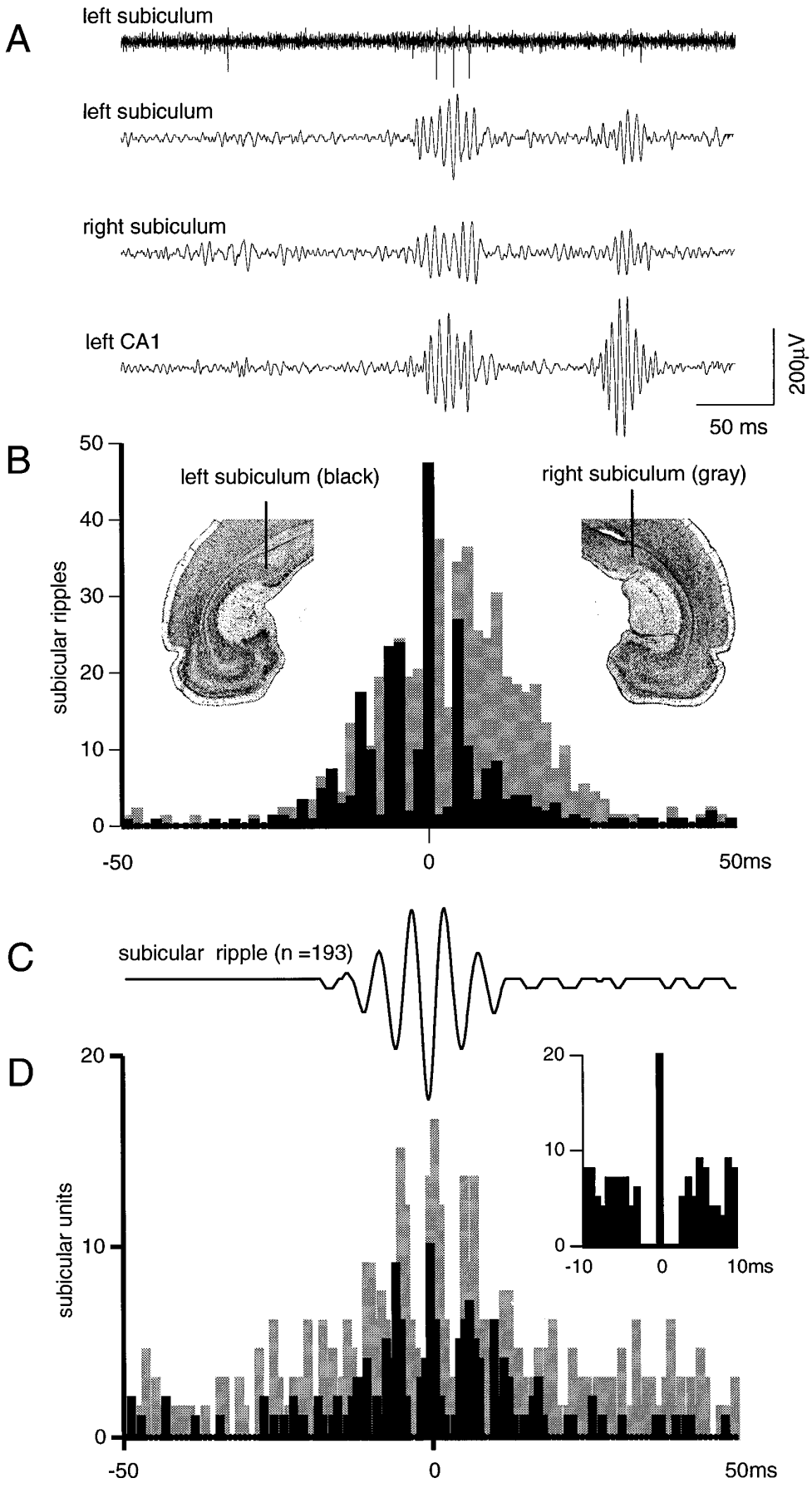

Figure 3. CA1 ripple and associated neuronal events in the ipsilateral and contralateral subiculum. *A,* Single 400 msec sweep with ripple doublets recorded at three sites and subicular unit. *B,* Cross-correlograms of ipsilateral (*black*) and contralateral (*gray*) subicular ripples to the peak of the CA1 reference ripple (n = 224 CA1 ripples). Note the prominent wave-by-wave coherence on the ipsilateral side and its absence in the contralateral subiculum. *Insets* in *B* illustrate position of electrodes in the dorsal subiculum (figures as from Swanson, 1992). *C,* Averaged subicular ripple (n = 193) and its relation to single (*black*) and multiunit (*gray*) activity recorded at the same site. *D,* Zero reference was negative peak of the local subicular ripple. *Inset* in *D,* autocorrelogram of single unit.

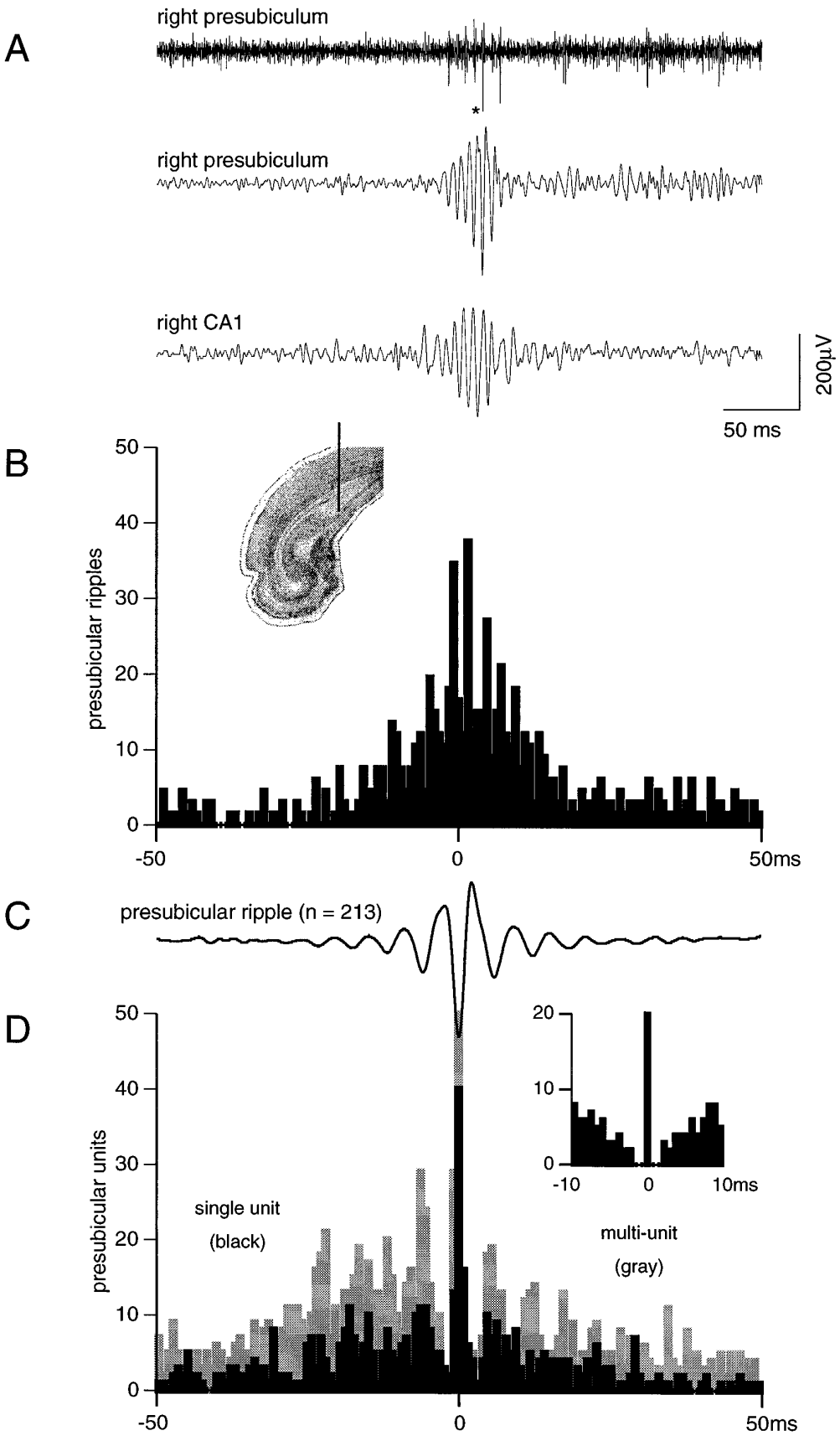

Figure 4. CA1 ripple and associated neuronal events in the deep layers of the ipsilateral presubiculum. *A,* Single 400 msec sweeps recorded from CA1 and the ipsilateral presubiculum. *Top trace* illustrates the discharge of a single (*) and multiunit presubicular neurons. *B,* Cross-correlogram of ipsilateral presubicular ripple to the peak of the CA1 reference ripple (n = 257 CA1 ripples). *Inset* in *B* illustrates position of electrode in the dorsal presubiculum. *C,* Averaged presubicular ripple (n = 213). *D,* Cross-correlograms of single (*black*) and multiunit (*gray*) activity and presubicular ripples; zero reference was negative peak of local presubicular ripple. *Inset* in *D,* Autocorrelogram of single unit.

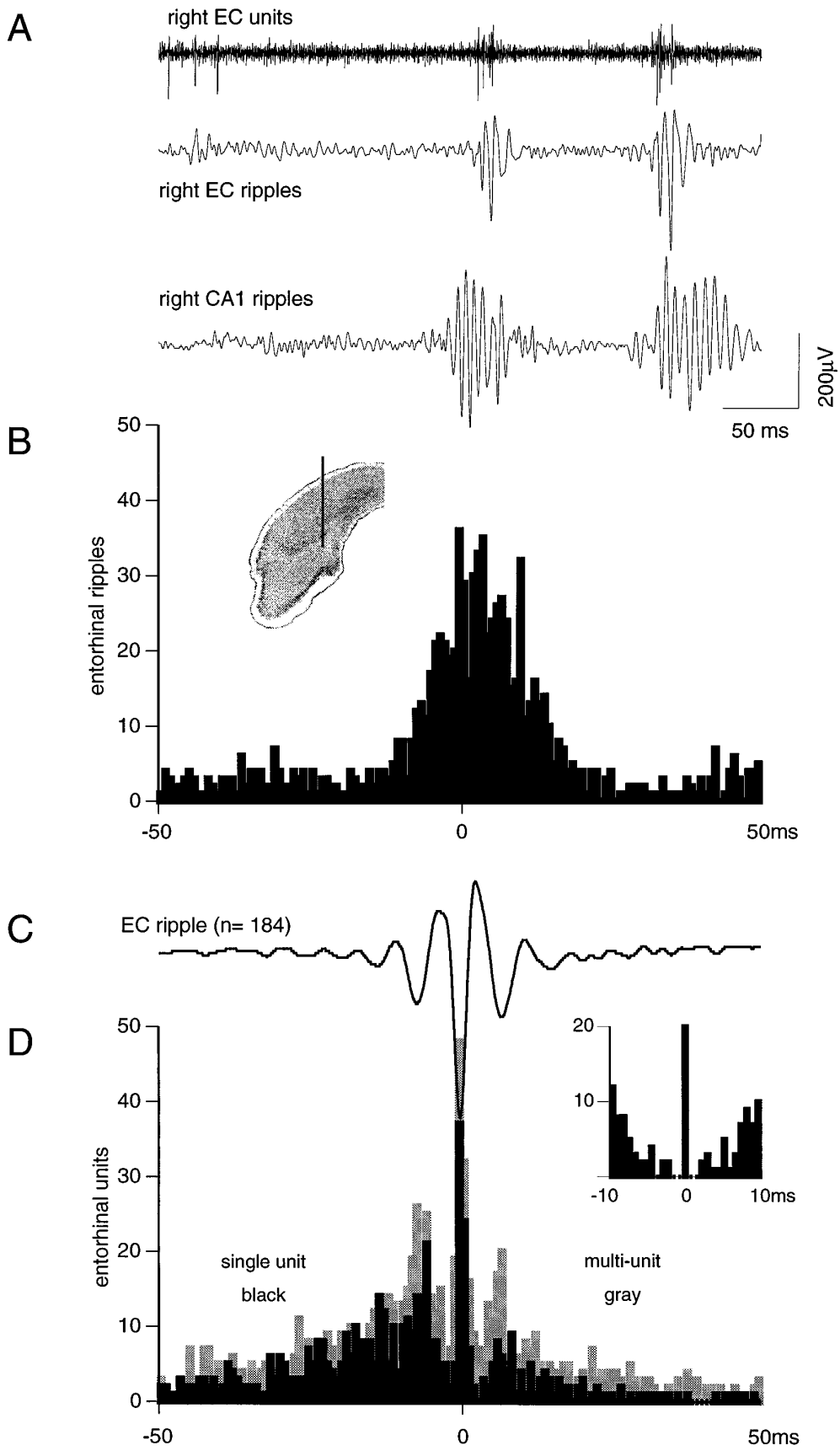

Figure 5. CA1 ripple and associated neuronal events in the deep layers of the ipsilateral entorhinal cortex. *A*, Single 400 msec sweeps with concurrent ripples in CA1 and the ipsilateral EC. *Top trace*, discharge of entorhinal neurons at the site where the entorhinal ripple was recorded. *B*, Cross-correlograms of the ipsilateral entorhinal ripple with the peak of CA1 ripple as zero reference (n = 211). Note the absence of ripple-related modulation in the cross-correlogram. *Inset* in *B* illustrates position of electrodes in the rostral EC. *C*, Averaged entorhinal ripple (n = 213). *D*, Cross-correlograms of single *(black)* and multiunit *(gray)* activity and entorhinal ripples; zero reference was negative peak of entorhinal ripple. *Inset* in *D*, Autocorrelogram of single unit.

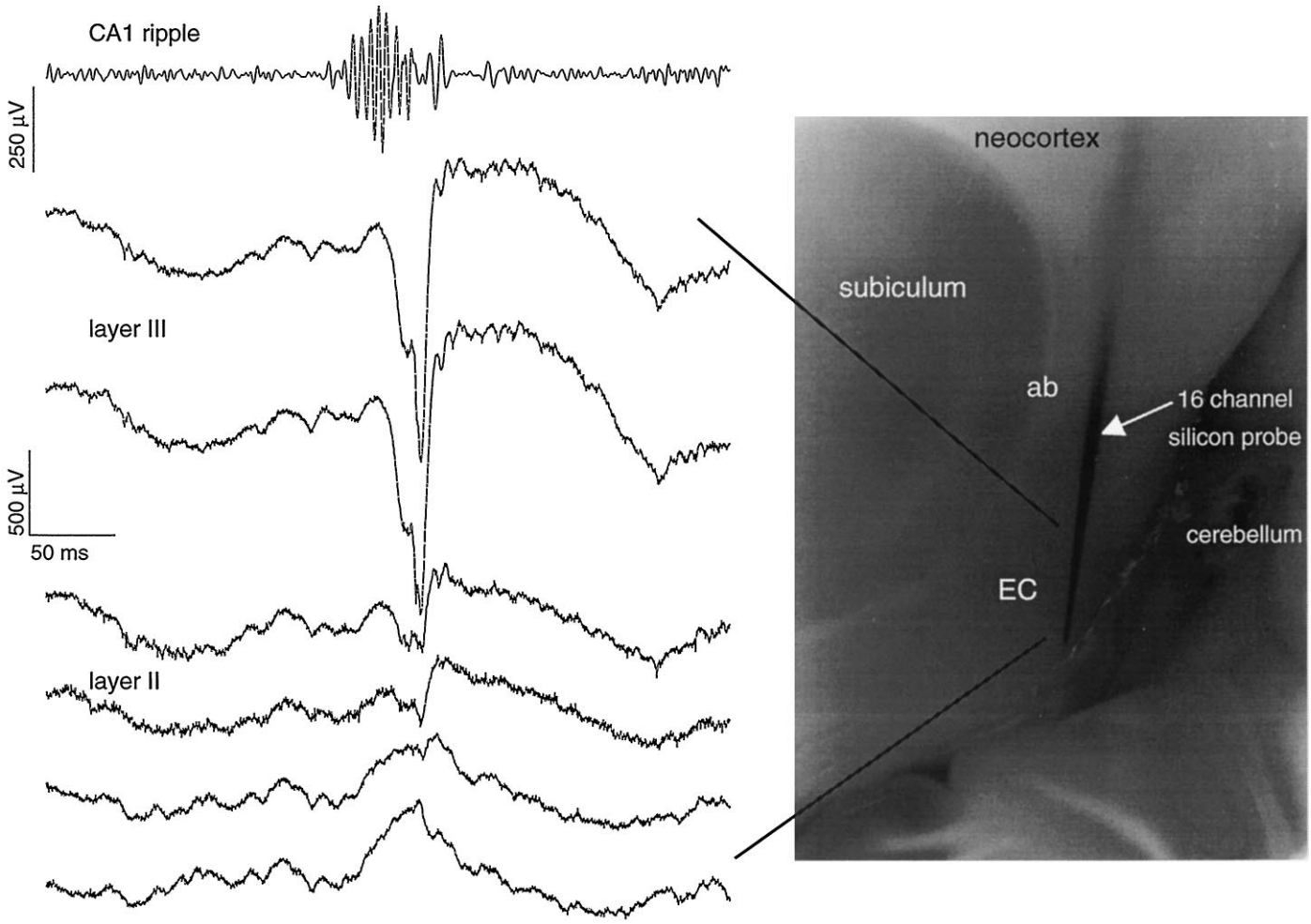

Figure 6. Depth profile of an entorhinal sharp wave and its relation to a CA1 ripple. A 16-channel silicon probe (*arrow*) was used to record concurrently at multiple laminar sites within the entorhinal cortex. The figure illustrates the relation of this large depolarizing input to the dendritic fields of layers V–VI and III neurons throughout the broad expanse of layers IV and III of the entorhinal cortex. Image (*right*) illustrates the position of the silicon probe with its tip near the superficial border of the *EC*. *ab*, Angular bundle.

close to, but below, discharge threshold. Although CA1 interneurons discharge near 200 Hz, CA1 pyramidal cells typically discharge once or not at all during a ripple. The discharge of CA1 pyramidal cells is thus highly constrained, despite a massive depolarization from the CA3 input.

We suggest that the locally developing field oscillations throughout the hippocampal–entorhinal output network develop in a manner analogous to that observed in CA1. Thus, feed-forward excitation simultaneously drives low-threshold networks of interneurons that discharge at a high frequency, whereas pyramidal cells discharge in population bursts: the population burst driven by feed-forward excitation, but concurrently constrained by the influence of the local interneuron barrage. The high degree of transient synchrony observed throughout the network is likely to reflect the anatomical arrangement of (1) feed-forward excitatory projections and/or (2) long-range inhibitory projections. Coupling across regions may be achieved by GABAergic interneurons with wide-ranging axon collaterals (Sik et al., 1995) and/or gap junctions, and such interneuronal "supernetworks" may co-operatively entrain large populations of pyramidal cells in the hippocampal–entorhinal axis (Buzsáki and Chrobak, 1995).

Fast oscillations within the hippocampal/retrohippocampal output pathways during sharp waves: coordinated activity in a distributed neural network

The temporally coordinated activity of neurons within spatially distributed networks is an important functional unit within the nervous system (Hebb, 1949; Konorski, 1949). Rhythmic field potentials reflect temporal frameworks for synchronizing neural activity, i.e., for bringing neuroanatomically distributed and sparsely connected neurons together in time (Buzsáki et al., 1983; Steriade et al., 1990, 1993; Gray, 1994). Although sharp waves are aperiodic, they are associated with a high-frequency oscillation within the entire hippocampal–entorhinal output network. Synchronized neural discharges occur within this large network during these events. It is important to note that synchronized oscillations and unit discharges do not occur throughout the entire network with each and every sharp wave; rather they emerge within varying topographical locations and involve varying subpopulations of neurons. The degree of synchronization between any two sites within the network varies from event to event and is likely to reflect anatomical/synaptic connectivity. Clearly, the degree of synchronization across the dorsal CA1 and adjacent sub-

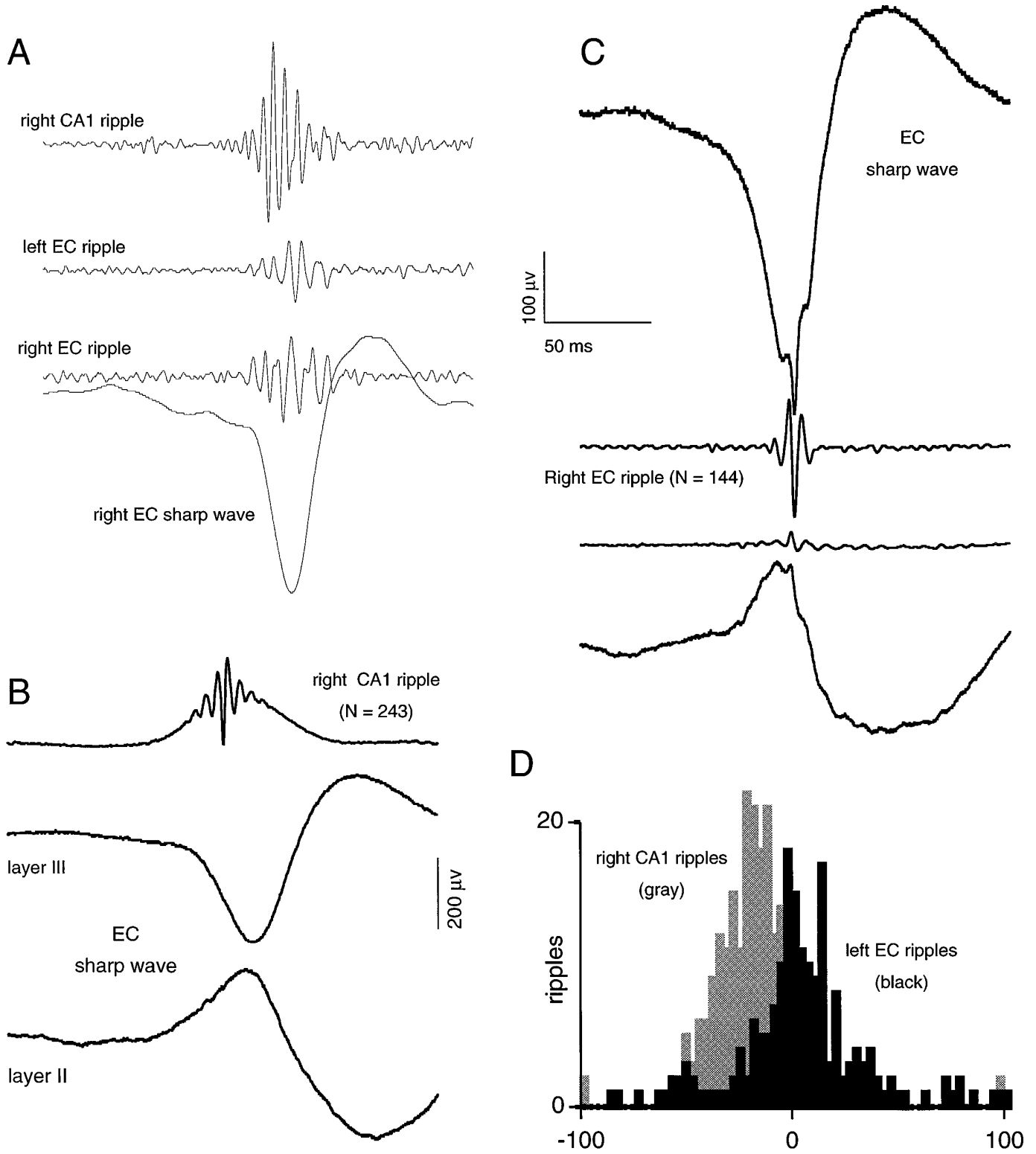

Figure 7. CA1 ripple and associated high-frequency oscillations in the EC. *A,* Single 400 msec sweeps with concurrent ripples in the CA1 region and both hemispheres of the EC. Note the time lag and lower frequency of the entorhinal oscillations. *B,* Averaged extracellular fields (*wide band*) in the hippocampus and ipsilateral EC triggered by the negative peak of CA1 ripples ($n = 243$). *Top trace* is average extracellular fields in stratum oriens. *Bottom traces* are averaged entorhinal sharp waves illustrating reversal near the border of layers II–III. *C,* Average extracellular fields in the same EC locations triggered by the negative peak of the entorhinal high-frequency oscillation. *Top* and *bottom traces* (1–5 kHz) are layers III and II sites as shown in *B,* respectively. *Middle traces* are the same sites filtered (100–400 Hz) for ripples. Note reversal of high-frequency oscillation. *D,* Relation of contralateral entorhinal ripples (*black*) and ipsilateral CA1 ripples (*gray*) to the negative peak of the ipsilateral entorhinal ripple (same zero reference as *C*).

icular region, over many ripple events, is much greater within any given hemisphere as compared with the contralateral hemisphere (Figs. 1–3) or ipsilateral retrohippocampal sites (Figs. 4–6). As suggested above, the degree of synchronization within/across regions may reflect the anatomical interconnectivity of interneuronal networks. In this regard, it is important to appreciate the extensive interconnectivity of GABAergic interneurons within the CA1 region (Sik et al., 1995), the lack of substantial interconnections among CA1 pyramidal neurons (Christian and Dudek, 1988; Thomson and Radpour, 1991), and the lack of any significant contralateral projections from either CA1 interneurons or pyramidal neurons (Amaral and Witter, 1995).

Bringing neurons within the hippocampal–retrohippocampal network together in time on such a short time-scale provides a potent means of enhancing their impact on common postsynaptic targets. If convergent activation of neurons is related to potentiating synaptic efficacy (Bliss and Lømo, 1973; Bliss and Collinridge, 1993), then the convergent activity of the hippocampal–entorhinal output network is a potent, *endogenous,* means for modifying the synaptic connectivity within this network and in its anatomical targets throughout the forebrain.

Relevance of hippocampal–entorhinal population oscillations to cognitive/computational processes

We have suggested that formation and consolidation of memories within this network involves two distinct companion processes (Buzsáki, 1989; Chrobak and Buzsáki, in press). The initial transfer of information into the circuitry of the hippocampus is thought to be supported by θ-modulated γ oscillations within the entorhinal–dentate axis and at their targets within CA3–CA1 (Bragin et al., 1995; Chrobak and Buzsáki, 1995; in press). This on-line modification of preexistent network connectivity serves as a means of imprinting information on the output circuitry of the hippocampus. Free from the ongoing transfer of input into its circuitry, the CA3-CA1-retrohippocampal network then engages in synaptic modification of its own and target neocortical networks. The synchronization of the output circuitry associated with each sharp-wave burst is thought to play a fundamental role in a protracted consolidation process, "whereby medial temporal lobe structures direct the gradual establishment of memory representations in neocortex" (Squire and Alvarez, 1995; also see Marr, 1971). This general framework is compatible with a considerable volume of evidence documenting the temporal gradient of retrograde amnesia associated with temporal lobe insult (Ogden and Corkin, 1991; Squire, 1992; Cho et al., 1993; Kim et al., 1995). This literature demonstrates that the hippocampal–entorhinal substrates participate in a consolidation process that takes place after the acquisition of information and over a variable period of minutes, hours, days, weeks, and even many months transfers representations, or access to representations, to a neocortical substrate. This framework is also compatible with recent multiunit recordings in freely behaving rats demonstrating correlated neural activity among pairs of neurons as a consequence of recent experience that is maintained during subsequent sleep periods (Wilson and McNaughton, 1994; Kudrimoti et al., 1995), as well as theoretical modeling studies that have examined the relative efficiency of this dual-process approach for modifying neural networks (McClelland et al., 1995).

We suggest that the major physiological role of this organized network burst is long-term alterations in synaptic efficacy. The synchronized 200 Hz discharge of the hippocampal–entorhinal output network (1) occurs within the appropriate anatomical pathway, so as to convey the outcome of hippocampal processing to neocortical networks, (2) occurs within a logical time domain, so as to be relevant to an "after the fact" consolidation process, and (3) may provide the prerequisite depolarizing force needed to produce synaptic modifications of neocortical networks.

Entorhinal sharp waves: the impact of the output network on the input (layers II–III) network

Cells within the deep layers of the presubiculum and parasubiculum appear continuous with the principal cell layer of the subiculum and the deep layers of the EC (Amaral and Witter, 1995). Our present findings support the continuity of this functionally integrated output network.

Previous findings demonstrated that the superficial layer (II–III) neurons within these regions do not seem to be influenced by hippocampal sharp waves (Chrobak and Buzsáki, 1994). Anatomical circuits exist for the activation of layer II–III neurons by the hippocampal–entorhinal output network, which would then allow for reentrant activation of the hippocampus via the perforant path; however, the physiological activity of this circuitry seems to be constrained powerfully by dominant inhibitory influences within the superficial layers (Finch et al., 1986, 1988; Jones and Heinemann, 1988; Bartesaghi et al., 1989; Jones and Lambert, 1990; Jones and Buhl, 1993; Chrobak and Buzsáki, 1995; Paré et al., 1995). This dominant inhibition, however, may provide mechanisms for a circumscribed activation of superficial layer neurons, and this possibility is under investigation. On the other hand, a general compromise of this inhibition would expose this circuitry to an unaccustomed excitatory barrage. Failure of inhibition at this critical juncture is likely to play a prominent role in the transition of physiological network bursting to pathophysiological reverberating epileptiform activity (Paré et al., 1992; Jones, 1993). We believe that understanding the basic physiology of this intricate neural machinery at the level of an operational system is essential for describing the neural substrate of memory formation as well as the pathological dysfunction of this substrate as manifest in temporal lobe epilepsy and Alzheimer's dementia.

REFERENCES

Amaral DG, Witter MP (1995) Hippocampal formation. In: The rat nervous system, 2nd Ed (Paxinos G, ed), pp 443–493. Los Angeles: Academic.

Bartesaghi R, Gessi T, Sperti L (1989) Electrophysiological analysis of the hippocampal projections to the entorhinal area. Neuroscience 30:51–62.

Bliss TVP, Lømo T (1973) Long-lasting potentiation of synaptic transmission in the dentate area of the anaesthetized rabbit following stimulation of the perforant path. J Physiol (Lond) 232:331–356.

Bliss TVP, Collinridge GL (1993) A synaptic model of memory: long-term potentiation in the hippocampus. Nature 361:31–39.

Boeijinga PH, Lopes da Silva FH (1988) Differential distribution of β and ø EEG activity in the entorhinal cortex of the cat. Brain Res 448:272–286.

Bragin A, Jando G, Nadasdy Z, Hetke J, Wise K, Buzsáki G (1995) Gamma (40–100 Hz) oscillation in the hippocampus of the behaving rat. J. Neurosci 15:47–60.

Buzsáki G, Chrobak JJ (1995) Temporal structure in spatially organized neuronal ensembles: a role for interneuron networks. Curr Opin Neurobiol 5:504–510.

Buzsáki G (1986) Hippocampal sharp waves: their origin and significance. Brain Res 398:242–353.

Buzsáki G (1989) Two-stage model of memory trace formation: a role for "noisy" brain states. Neuroscience 31:551–570.

Buzsáki G, Bickford RG, Ryan LJ, Young S, Prohaska O, Mandel RJ, Gage FH (1989) Multisite recording of brain field potentials and unit activity in freely moving rats. J Neurosci Methods 28:209–217.

Buzsáki G, Leung LS, Vanderwolf CH (1983) Cellular basis of hippocampal EEG in the behaving rat. Brain Res 6:139–171.

Buzsáki G, Horváth Z, Urioste R, Hetke J, Wise K (1992) High frequency network oscillation in the hippocampus. Science 1025–1027.

Cho YH, Beracochea D, Jaffard R (1993) Extended temporal gradient for the retrograde and anterograde amnesia produced by ibotenate entorhinal cortex lesions in mice. J Neurosci 12:1759–1766.

Christian EP, Dudek FE (1988) Electrophysiological evidence from glutamate microapplications for local excitatory circuits in the CA1 area of rat hippocampal slices. J Neurophysiol 59:110–123.

Chrobak JJ, Buzsáki G (1994) Selective activation of deep layer (V–VI) retrohippocampal cortical neurons during hippocampal sharp waves in the behaving rat. J Neurosci 14:6160–6170.

Chrobak JJ, Buzsáki G (1995) Temporal structure in the discharge of superficial layer (II–III) entorhinal cortical neurons. Soc Neurosci Abstr 21:1206.

Chrobak JJ, Buzsáki G (1996) Entorhinal–hippocampal network dynamics constrain synaptic potentiation and memory formation. In: Long-term potentiation: current issues (Baudry M, Davies JL, eds). Cambridge: MIT, in press.

Finch DM, Wong EE, Derian EL, Babb TL (1986) Neurophysiology of limbic system pathways in the rat: projections from the subicular complex and hippocampus to the entorhinal cortex. Brain Res 397:205–213.

Finch DM, Tan AM, Isokawa-Akesson M (1988) Feedforward inhibition of the rat entorhinal cortex and subicular complex. J Neurosci 8:2213–2226.

Fox SE (1989) Membrane potential and impedance changes in hippocampal pyramidal cells during theta rhythm. Exp Brain Res 41:283–294.

Freeman W, Barrie JM (1994) Chaotic oscillations and the genesis of meaning in cerebral cortex. In: Temporal coding in the brain (Buzsáki G, Llinas RR, Singer W, Berthoz A, Christen Y, eds), pp 13–37. New York: Springer.

Gallyas F, Guldner FH, Zoltay G, Wolff JR (1990) Golgi-like demonstration of "dark"neurons with an argyrophil III method for experimental neuropathology. Acta Neuropathol (Berl) 79:620–628.

Gray CM (1994) Synchronous oscillations in neuronal systems: mechanisms and functions. Comp Neurosci 1:11–38.

Hebb DO (1949) The organization of behavior. New York: Wiley.

Jones RSG, Heinemann U (1988) Synaptic and intrinsic responses of medial entorhinal cortical cells in normal and magnesium-free medium in vitro. J Neurophysiol 59:1476–1496.

Jones RSG (1993) Entorhinal–hippocampal connections: a speculative view of their function. Trends Neurosci 16:58–64.

Jones RSG, Lambert JDC (1990) The role of excitatory amino acid receptors in the propagation of epileptiform discharges from the entorhinal cortex to the dentate gyrus in vitro. Exp Brain Res 80:310–322.

Jones RSG, Buhl EH (1993) Basket-like interneurons in layer II of the entorhinal cortex exhibit a powerful NMDA-mediated synaptic excitation. Neuroscience 149:35–39.

Kim JJ, Clark RE, Thompson RF (1995) Hippocampectomy impairs the memory of recently, but not remotely acquired trace eyeblink conditioned responses. Behav Neurosci 109:195–203.

Konorski J (1949) Integrative activity of the brain. Chicago: The University of Chicago.

Kudrimoti HS, McNaughton BL, Barnes CA, Skaggs WE (1995) Recent experience strengthens pre-existing correlations between hippocampal neurons during sleep. Soc Neurosci Abstr 21:941.

Leung LS, Yim CY (1986) Intracellular records of theta rhythm in hippocampal CA1 cells of the rat. Brain Res 367:323–327.

Marr D (1971) Simple memory: a theory for archicortex. Philos Trans R Soc Lond [Biol] 262:23–81.

McClelland JL, McNaughton BL, O'Reilly RC (1995) Why there are complementary learning systems in the hippocampus and neocortex: insights form the successes and failures of connectionist models of learning and memory. Psychol Rev 102:419–457.

Michelson HB, Wong RKS (1994) Synchronization of inhibitory neurons in the guinea-pig hippocampus in vitro. J Physiol (Lond) 477:35–45.

Mitchell SJ, Ranck JB (1980) Generation of theta rhythm in medial entorhinal cortex of freely moving rats. Brain Res 189:49–66.

Ogden JA, Corkin A (1991) Memories of HM. In: Memory mechanisms: a tribute to G.V. Goddard (Abraham WC, Corballis MC, White KG, eds), pp 195–218. Hillsdale, NJ: Lawrence Erlbaum Associates.

Paré D, Ong J, Gaudreau H (1995) Amygdalo-entorhinal relations and their reflection in the hippocampal formation: generation of sharp sleep potentials. J Neurosci 15:2482–2503.

Paré D, deCurtis M, Llinás R (1992) Role of hippocampal–entorhinal loop in temporal lobe epilepsy: extra- and intracellular study in the isolated guinea pig brain *in vitro.* J Neurosci 12:1867–1881.

Sik A, Penttonen M, Ylinen A, Buzsáki G (1995) Hippocampal CA1 interneurons: an *in vivo* intracellular labeling study. J Neurosci 6651–6665.

Singer W (1994) Time as coding space in neocortical processing: a hypothesis. In: Temporal coding in the brain (Buzsáki G, Llinas RR, Singer W, Berthoz A, Christen Y, eds), pp 251–272. New York: Springer.

Soltész I, Deschénes M (1993) Low- and high-frequency membrane potential oscillations during theta activity in CA1 and CA3 pyramidal neurons of the rat hippocampus under ketamine-xylazine anesthesia. J Neurophysiol 70:97–116.

Squire L, Alvarez P (1995) Retrograde amnesia and memory consolidation: a neurobiological perspective. Curr Opin Neurobiol 5:169–177.

Squire L (1992) Memory and the hippocampus: a synthesis from findings with rats, monkeys and humans. Psychol Rev 99:195–231.

Steriade M, McCormick DA, Sejnowski TJ (1993) The sleeping and aroused brain: thalamocortical oscillations in neurons and networks. Nature 262:679–685.

Steriade M, Gloor P, Llinás RR, Lopes de Silva FH, Mesulam M-M (1990) Basic mechanisms of cerebral rhythmic activities. Electroencephalogr Clin Neurophysiol 76:481–508.

Stewart M, Quirk GJ, Barry M, Fox SE (1992) Firing relation of medial entorhinal neurons to the hippocampal theta rhythm in urethane anesthetized and walking rats. Exp Brain Res 90:21–28.

Suzuki SS, Smith GK (1987) Spontaneous EEG spikes in the normal hippocampus: I. Behavioral correlates, laminar profiles and bilateral synchrony. Electroencephalogr Clin Neurophysiol 67:438–459.

Swanson LW (1992) Brain maps: structure of the rat brain. Amsterdam: Elsevier.

Thomson AM, Radpour S (1991) Excitatory connections between CA1 pyramidal cells revealed by spike-triggered averaging in slices of rat hippocampus are partially NMDA-receptor mediated. Eur J Neurosci 3:587–601.

Traub RD, Whittington MA, Colling SB, Buzsáki G, Jefferys JGR (1996) Analysis of gamma rhythms in the rat hippocampus in vitro and in vivo. J Physiol (Lond), in press.

Wilson M, McNaughton BL (1994) Reactivation of hippocampal ensemble memories during sleep. Science 265:676–679.

Ylinen A, Sik A, Bragin A, Nadásdy Z, Jandó G, Szabó I, Buzsáki G (1995) Sharp wave-associated high-frequency oscillation (200 Hz) in the intact hippocampus: network and intracellular mechanisms. J Neurosci 15:30–46.

Whittington MA, Traub RD, Jeffreys JGR (1995) Metabotropic receptor activation drive synchronized 40 Hz oscillations in networks of inhibitory neurons. Nature 373:612–615.